Journal of Cellular Biochemistry 104:756–772 (2008)

S1P-Lyase Independent Clearance of Extracellular Sphingosine 1-Phosphate After Dephosphorylation and Cellular Uptake

Ulrike Peest,[1] Sven-Christian Sensken,[1] Paul Andréani,[1] Petra Hänel,[1] Paul P. Van Veldhoven,[2] and Markus H. Gräler[1]*

[1]Institute for Immunology, Hannover Medical School, Carl-Neuberg-Str. 1, 30625 Hanover, Germany
[2]Laboratory for Lipid Biochemistry and Protein Interactions, Department of Molecular Cell Biology, K.U.Leuven, Herestraat 49, 3000 Leuven, Belgium

Abstract Sphingosine 1-phosphate (S1P) is the natural ligand for a specific family of G protein-coupled receptors (-Rs). The type 1 S1P-R ($S1P_1$) is important for lymphocyte egress, and blood-borne S1P as the natural ligand for $S1P_1$ is involved in the maintenance of lymphocyte circulation. This report reveals that extracellular S1P was cleared by all tested primary cells and cell lines with exponential progression. Clearance of S1P, but not sphingosine (Sph) was inhibited with the protein phosphatase inhibitor sodium orthovanadate. Fluorescence microscopy and flow cytometry using fluorescently labeled S1P and Sph showed a major cellular uptake of Sph, but not S1P. HPLC-analyses with C17-Sph demonstrated that cellular Sph accumulation was transient in tested cell lines, but enduring in mouse splenocytes. Sub cellular fractionation resulted in dephosphorylation of S1P to Sph by nuclear, membrane, and cytosolic fractions. Degradation of Sph however only occurred in combined membrane and cytosolic fractions. Inhibitors for Sph kinases 1/2, ceramide synthase, and S1P-lyase, as well as S1P-lyase deficiency did not block clearance of extracellular S1P. In vivo experiments revealed a transient increase in plasma S1P levels after single intravenous injection into C57BL/6 mice. This exogenously added S1P was cleared within 15–30 min in contrast to ex vivo incubation of whole blood which required more than 8 h for comparable clearance from plasma. Our data thus show that extracellular S1P is dephosphorylated and subsequently converted by cells, which appears to be important for clearance of the signaling molecule S1P in the local tissue environment after infections or injuries. J. Cell. Biochem. 104: 756–772, 2008.

Key words: sphingolipid; lymphocyte; blood; sphingosine kinase; S1P-lyase; ceramide synthase

Sphingosine 1-phosphate (S1P) is a bioactive lipid with various functional capabilities. Intracellularly it is crucial for cell survival [Cuvillier et al., 1996]. S1P is thought to be an intracellular second messenger, although the intracellular target molecule for S1P has not yet been identified [Meyer zu Heringdorf et al., 2003]. Over the past years it became evident that S1P is also active as a ligand for five cell surface G protein-coupled receptors designated $S1P_{1-5}$

This article contains supplementary material, which may be viewed at the Journal of Cellular Biochemistry website at http://www.interscience.wiley.com/jpages/0730-2312/suppmat/index.html.

Abbreviations used: S1P, sphingosine 1-phosphate; Sph, sphingosine; DH-S1P, dihydro-sphingosine 1-phosphate; DH-Sph, dihydrosphingosine; DMS, dimethylsphingosine; DOP, 4-deoxypyridoxine; FuB1, fumonisin B1; PI, phosphatase inhibitor mix (2 mM imidazole (I), 1 mM sodium fluoride (SF), 1.15 mM sodium molybdate (SM), 1 mM sodium orthovanadate (SOV), and 4 mM sodium tartrate (ST)); FMOC-Cl, 9-fluorenylmethylchloroformiate; HPLC, high performance liquid chromatography; FITC, fluorescein isothiocyanate.

Grant sponsor: German Research Foundation (DFG); Grant number: GR 1943/1-3.

*Correspondence to: Dr. Markus H. Gräler, Institute for Immunology, Hannover Medical School, OE 9422, Bldg. K11, Carl-Neuberg-Str. 1, 30625 Hanover, Germany.
E-mail: graeler.markus@mh-hannover.de

Received 1 August 2007; Accepted 14 November 2007
DOI 10.1002/jcb.21665

[An et al., 1997; Lee et al., 1998; Im et al., 2000; Van Brocklyn et al., 2000; Chun et al., 2002]. Although the physiological role of most of these receptors is still enigmatic, expression of the $S1P_1$-receptor on thymocytes and naive lymphocytes was recently shown to be important for their exit from thymus and from secondary lymphoid organs (SLOs) respectively [Gräler and Goetzl, 2002; Gräler et al., 2002; Allende et al., 2004; Matloubian et al., 2004]. This observation suggests that S1P as the natural ligand for the $S1P_1$-receptor plays a crucial role for the maintenance of lymphocyte circulation [Gräler and Goetzl, 2004]. S1P is present in blood up to micromolar concentrations [Yatomi et al., 1997; Ruwisch et al., 2001]. It was reported that cells, especially thrombocytes produce and secrete S1P after stimulation [Yatomi et al., 2000; English et al., 2000a]. But this mechanism is most likely involved in transient S1P secretion in the microenvironment of peripheral tissues during infection or injury and does not account for the basal levels observed in blood. We recently identified erythrocytes as a major source for S1P in blood [Hänel et al., 2007]. Regulation of S1P secretion and degradation is important in both local and systemic environments. Locally S1P is an anti-inflammatory mediator that is released during an infection [Cummings et al., 2002; Roviezzo et al., 2004]. Activated mast cells are at least one source for secreted S1P during inflammation [Jolly et al., 2004]. S1P is also known as a stimulator for wound repair after injury [Lee et al., 2000]. Activated thrombocytes were described as a major source for extracellular S1P to facilitate healing [English et al., 2000b]. In both situations an inducible release and rapid clearance of extracellular S1P in the local environment ensure a transient cell activation which is mediated by S1P receptor stimulation.

This study investigated the fate of S1P during in vitro culture with cell lines including rat hepatoma HTC_4 cells, human embryonic kidney HEK293 cells, mouse B lymphoma LK35.2 cells, and human T lymphoma Jurkat cells, during ex vivo culture of primary mouse splenocytes, and in vivo after single intravenous injection of 1 mg/kg S1P into wild-type C57BL/6 mice. For S1P and Sph detection we used a newly developed high performance liquid chromatography (HPLC) method.

MATERIALS AND METHODS

Chemicals, Cell Lines, and Mice

Sphingolipids were purchased from Sigma–Aldrich (Taufkirchen, Germany) except for N,N-dimethylsphingosine and D-erythro- sphingosine that were purchased from Alexis (Grünberg, Germany). C17-S1P and C17-Sph were purchased from Otto Nordwald GmbH (Hamburg, Germany), S1P-FITC and Sph-FITC were from Tebu-Bio (Offenbach, Germany). Sphingolipids were added directly from 1 mM stock solutions in methanol. For final concentrations above 1 μM, the solvent was evaporated first, and the sphingolipids were redissolved in the appropriate medium after sonicating in a water bath sonicator and vigorous vortexing. Chemicals and solvents were purchased from Roth (Karlsruhe, Germany) if not stated otherwise. Human embryonic kidney HEK293 cells (ATCC, CRL-1573), the human T lymphoma cell line Jurkat (ATCC, TIB-152), the mouse B cell hybridoma line LK35.2 (ATCC, HB98), and rat hepatoma HTC_4 cells were cultured as described [Gräler and Goetzl, 2004]. Mouse splenocytes were isolated and cultured according to standard protocols [Gräler and Goetzl, 2004]. Cell culture media and supplements were purchased from PAA (Cölbe, Germany). C57BL/6 mice were purchased from the Hannover Medical School Animal Facility (Hanover, Germany). S1P-lyase deficient mice were generated as described [Van Veldhoven, 2005].

Lipid Extraction

Biological samples (1 ml medium, 5×10^6 cells, 10–30 mg tissue, 100 μl serum or plasma) were adjusted to 1 ml sample volume with 1 M NaCl and transferred into a glass centrifuge tube. After addition of 1 ml methanol (Baker; Griesheim, Germany) and 200 μl of 18.5% hydrochloric acid the samples were vortexed. Two milliliters of chloroform was added, and the samples were vigorously vortexed for 2 min. Samples were centrifuged for 3 min at $1{,}900 \times g$, and the lower chloroform phase was transferred into a new glass centrifuge tube. After repeating the lipid extraction with another 2 ml of chloroform, the two chloroform phases were combined and vacuum-dried in a speed-vac for 45 min at 48°C.

Derivatization of Sphingolipids With 9-Fluorenylmethylchloroformiate (FMOC-Cl)

Eighteen milligrams of FMOC-Cl were dissolved in 5 ml dioxane. Vacuum-dried samples

were dissolved in 200 μl dioxane with subsequent addition of 200 μl of 70 mM dipotassiumhydrogenphosphate in H_2O and 200 μl FMOC-Cl solution [Andréani and Gräler, 2006].

HPLC-Analysis of Fluorescently Labeled Sphingolipids

Chromatographic detection of sphingolipids was performed as described [Andréani and Gräler, 2006] using the Merck-Hitachi Elite LaChrom System (VWR; Darmstadt, Germany). The injection-pump delivery rate was 1.3 ml/min. The eluent was methanol, 70 mM dipotassiumhydrogenphosphate, and H_2O, forming a gradient over a period of 68 min for FMOC-labeled sphingolipids (Table I), and 30 min for FITC-labeled sphingolipids (Table II). Sample volume (10–100 μl) was injected using the Cut-injection method. Separation of sphingolipids with reversed-phase chromatography was done using a 250 × 4.6 mm Kromasil 100-5 C18 separation column and a 17 × 4 mm Kromasil 100-5 C18 precolumn (CS Chromatographie Service; Langerwehe, Germany). Column temperature was 35°C, detection was performed with a fluorescence detector at 263 nm excitation and 316 nm emission wavelengths for FMOC-labeled sphingolipids, and 494 nm excitation and 518 nm emission for FITC-labeled sphingolipids.

Splenocyte Isolation

Spleens from mice were minced on ice and pushed through a 70 μm mesh. Red blood cells were lysed in 138 mM NH_4Cl, 1 mM $KHCO_3$, and 0.1 mM EDTA for 5 min, and remaining splenocytes were washed three times with PBS supplemented with 10% FCS.

TABLE I. Gradient Table for FMOC-labeled Sphingolipids

Time (min)	Methanol (%)	70 mM K_2HPO_4 (%)	H_2O (%)
0	82	9	9
10	84	8	8
25	86	7	7
30	88	6	6
35	91	4.5	4.5
40	94	3	3
45	95	0	5
68	95	0	5

TABLE II. Gradient Table for FITC-Labeled Sphingolipids

Time (min)	Methanol (%)	70 mM K_2HPO_4 (%)	H_2O (%)
0	60	10	30
10	68.5	7.5	24
15	95	0	5
30	95	0	5

Flow Cytometry

Splenocytes and trypsinized HTC_4 cells were incubated for 1–60 min with 1 μM S1P-FITC or 1 μM Sph-FITC. Subsequently cells were washed twice with ice-cold PBS and analyzed using the FACSCalibur (Becton-Dickinson, Heidelberg, Germany). Dead cells were stained with 10 μg/ml propidium iodide and excluded from the analysis.

Fluorescence Microscopy

HTC_4 cells were seeded on glass cover slips and incubated for 1 h at 37°C with 1 μM S1P-FITC or 1 μM Sph-FITC. They were washed three times and fixed with 5% paraformaldehyde in ice-cold PBS for 15 min. After mounting them on microscope slides with Moviol, cells were analyzed using the fluorescence microscope IX81 (Olympus, Hamburg, Germany) and the imaging software analySIS D.

Cell Fractionation

HTC_4 cells (4×10^7) were homogenized on ice with a Dounce homogenizer. Nuclei were pelleted by centrifugation at 300 × *g* and 4°C for 5 min and washed twice with ice-cold PBS. Cell membranes were sedimented by ultracentrifugation at 72,000 × *g* and 4°C for 30 min and washed twice with ice-cold PBS. The supernatant was taken as the cytosolic fraction. Total protein concentrations derived from 4×10^7 cells were 3.7 mg (membrane fraction), 5.9 mg (cytosolic fraction), and 6.2 mg (nuclear fraction). Incubations were performed with cell fractions derived from 6.7×10^6 cells or 0.6 mg membrane proteins, 1 mg cytosolic proteins, and 1 mg nuclear proteins in 1 ml PBS for 4 h. Accordingly protein concentrations were 0.6 mg/ml (membrane fractions), 1 mg/ml (cytosolic fractions), and 1 mg/ml (nuclear fractions). For successive incubations, resulting lipids of the first incubation were extracted with chloroform as outlined above, and resuspended in 1 ml volume of the second cell fraction.

Reverse Transcriptase-PCR (RT-PCR)

Total RNA was prepared from 1×10^7 HTC_4 cells with TRIzol reagent (Invitrogen, Karlsruhe, Germany) according to the supplied protocol. Generation of cDNA was performed with First Strand cDNA Synthesis Kit (Fermentas, St. Leon-Rot, Germany) using 2 μg of isolated total RNA and 0.5 μg of an 18-mer oligo(dT) primer. PCR amplification using Taq DNA polymerase (Fermentas, St. Leon-Rot, Germany) was performed with 10 pmol of primers for ceramide synthase 1 (forward GTG CCT GGA AGC TTC TGT TC, reverse CTG ACG TCA TGC AGG AAG AA), ceramide synthase 2 (forward GAA GCC AGC TGG AGA TTC AC, reverse CCA GCA GGT AGT CGG AAG AG), ceramide synthase 3 (forward AGA ATT CGC CAG AAG CAA AA, reverse GGC TCG AGA TAG TGC AAA GG), ceramide synthase 4 (forward TGC ATG ACT GCT CCG ACT AC, reverse CCT TCA GAA ACT GCC TCG TC), ceramide synthase 5 (forward CAG CTG GCC TTC TAC TGG TC, reverse GGC TAA TCC CTC CTG GGT AG), ceramide synthase 6 (forward CTG AAG AAC ACG GAG GAA GC, reverse TGC CTT GTA TTC CAC AAC CA), lipid phosphate phosphatase 1a/b (forward CAG CGA TGG CTA CAT TGA GA, reverse TGC GTA GCT CTG TCT GTT GG), lipid phosphate phosphatase 2 (forward TGG GGT CAT CAT CAC AGC TA, reverse AGC CCA CAT AGA TGG CAA AG), lipid phosphate phosphatase 3 (forward CTA CAG GTG CCG AGG AGA AG, reverse CCA TGT TGT GGT GAT TGC TC), S1P-lyase (forward AGA GGC AGA AAT CGT GAG GA, reverse TCT GCT GAA ATG CTG GTC AC), S1P phosphatase 1 (forward GGA CGT CAT TGC TGG ATT CT, reverse ACC GAA GAG TTT GCA GGC TA), S1P phosphatase 2 (forward TTC ACC CTC CTC ATC TCC AC, reverse TTG GTC AGG CCT AAA ACC AG), Sph kinase 1 (forward TCA GTC TGT CCT GGG GTT TC, reverse AAC ACT CCC CTC TGG TTC CT), Sph kinase 2 (forward GCC AAG AGC CAA GTC AGA AC, reverse GGC TGA AGT GGT TTC CAT GT). Primers were designed with Primer3 V0.4.0 based on following GenBank sequences: Ceramide synthase 1 (NM_001044230), ceramide synthase 2 (BC101876), ceramide synthase 3 (XM_001059767), ceramide synthase 4 (XM_221796), ceramide synthase 5 (XM_001063108), ceramide synthase 6 (XM_ 001058317), lipid phosphate phosphatase 1a (AF503609), lipid phosphate phosphatase 2 (AF503611), lipid phosphate phosphatase 3 (Y07783), S1P-lyase (NM_173116), S1P phosphatase 1 (XM_001080791) S1P phosphatase 2 (XM_237343), Sph kinase 1 (NM_133386), Sph kinase 2 (NM_001012066) (cycling conditions: 94°C for 4 min; (94°C for 1 min; 50°C for 1 min; 72°C for 1 min) × 35 cycles; 72°C for 6 min).

RESULTS

Clearance of Exogenously Added S1P and Sph, and the Effect of Different Phosphatase Inhibitors

S1P and Sph were added to different cultured cell lines including rat hepatoma HTC_4 cells, human embryonic kidney HEK293 cells, mouse B lymphoma LK35.2 cells, and human T lymphoma Jurkat cells at a constant concentration of 300 nM, and incubated for 18 h. Afterwards cells and medium were harvested and analyzed separately. All cell lines were able to metabolize extracellular S1P and Sph over time (Fig. 1A). Jurkat cells however showed a greatly diminished clearance of added S1P (Fig. 1A). Medium alone did not provoke Sph conversion (Fig. 1A). But S1P was partly dephosphorylated to Sph in medium supplemented with 10% fetal calf serum (FCS) (Fig. 1A). In all tested cell lines the intracellular S1P concentration was below 30 pmol/5 million cells (Fig. 1B). Except for the human T cell line Jurkat with less than 10 pmol Sph in 5 million cells all other cell lines had considerably more intracellular Sph than S1P with levels around 30–60 pmol in 5 million cells (Fig. 1B). Since both extracellular S1P and Sph were cleared by cells the next question was whether or not dephosphorylation of S1P to Sph was required for its metabolism. 300 nM S1P and Sph were added to cultured rat hepatoma HTC_4 cells in the presence of a mix of different phosphatase inhibitors and incubated for 18 h. Phosphatase inhibitors almost completely inhibited degradation of S1P whereas clearance of extracellular sphingosine (Sph) was not affected (Fig. 1C). Intracellular S1P levels increased significantly under treatment with phosphatase inhibitors in contrast to Sph levels which remained mostly unaltered (Fig. 1D). Incubation of HTC_4 cells under these conditions with C17-S1P did not result in cellular accumulation of C17-S1P. Therefore the observed cellular S1P-increase after treatment with phosphatase inhibitors must be due to decreased degradation of endogenously synthesized S1P. Comparison

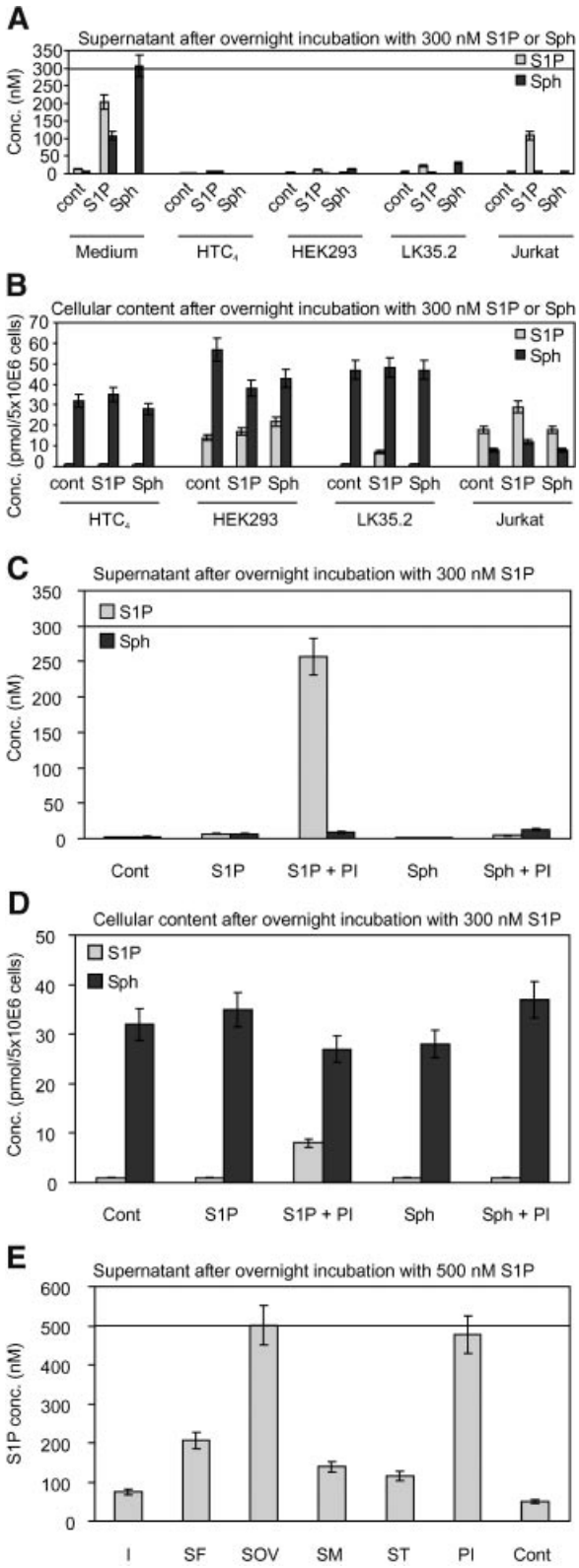

of single phosphatase inhibitors revealed that sodium orthovanadate, usually used as an inhibitor for protein phosphatases, was the most potent inhibitor of S1P metabolism which accounts for most if not all activity of the phosphatase inhibitor mix (Fig. 1E). Imidazole which inhibits alkaline phosphatase was ineffective (Fig. 1E). Acid phosphatase inhibitors like sodium fluoride, sodium molybdate, or sodium tartrate were also not able to inhibit S1P dephosphorylation and subsequent clearance (Fig. 1E).

Kinetics of S1P and Sph Degradation

Clearance of 300 nM S1P and Sph by HTC_4 cells was investigated over an 8 h period. S1P degradation followed an exponential regression, reaching the half maximal amount after 2 h (Fig. 2A). Clearance of Sph under the same conditions also followed an exponential decay (Fig. 2B). The half maximal amount was reached after 1 h. In both cases less than 10% were left in the medium after 8 h (Fig. 2A, B). Intracellular levels of Sph increased slightly during the first 60 min of the incubation period and did not change in the remaining 7 h (Fig. 2B). This increase may be explained at least in part by residual Sph sticking at the cell culture dish during cell harvesting. S1P-levels did not change intracellularly in the investigated time frame (Fig. 2A). To test the influence of endogenously produced S1P and Sph on the observed clearance of extracellular sphingolipids, C17-S1P and C17-Sph were added to HTC_4 cell cultures. C17-derivatives lack one hydrocarbon in their non-polar moiety compared to their natural analogs and are

Fig. 1. Metabolism of extracellular S1P and Sph by different cell lines and the effect of phosphatase inhibitors. **A**: Extracellular and (**B**) intracellular S1P and Sph levels after overnight incubation of 1 ml medium alone (Medium) and cultures of 5×10^6 HTC_4, HEK293, LK35.2, and Jurkat cells in 10 ml medium untreated (Cont) and after addition of 300 pmol/ml S1P and Sph. **C**: Extracellular and (**D**) intracellular levels of S1P and Sph after overnight incubation of 5×10^6 HTC_4 cells in 10 ml medium untreated (Cont) and after addition of 300 nM S1P and Sph in the presence of a phosphatase inhibitor mix (2 mM imidazole (I), 1 mM sodium fluoride (SF), 1.15 mM sodium molybdate (SM), 1 mM sodium orthovanadate (SOV), and 4 mM sodium tartrate (ST)) when indicated (PI). **E**: Extracellular S1P concentrations of 5×10^6 HTC_4 cells in 10 ml medium treated with 500 pmol/ml S1P and incubated overnight without (Cont) or with different phosphatase inhibitors as mentioned above. Each experiment was done two–three times. Error bars represent errors of the validated detection method.

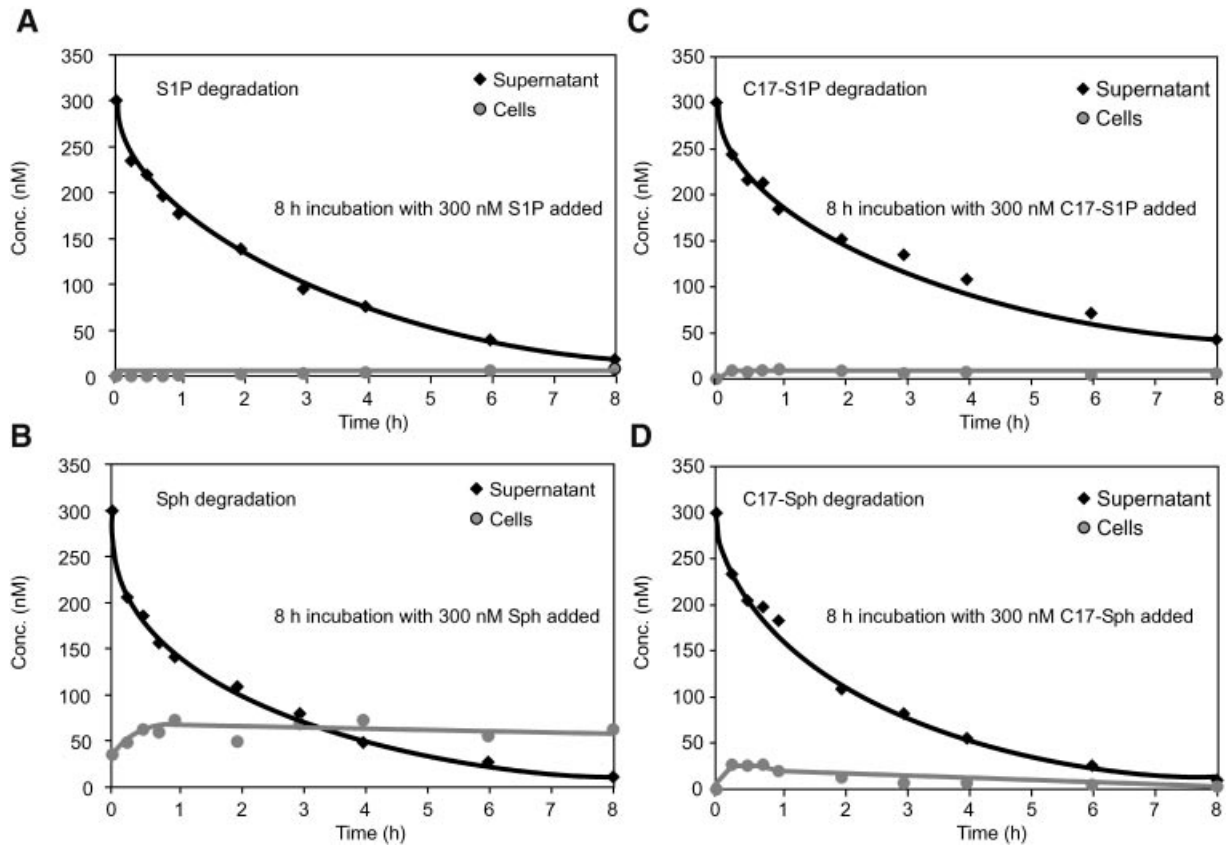

Fig. 2. Kinetics of extracellular S1P and Sph clearance. **A**: 300 nM of extracellularly added S1P, (**B**) Sph, (**C**) C17-S1P, and (**D**) C17-Sph were metabolized by 5×10^6 adherently grown HTC_4 cells in 10 ml medium over an 8 h period. Extracellular concentrations (Supernatant) as well as intracellular concentrations (Cells) of added sphingolipids after indicated incubation times are shown. Each experiment was done three times.

therefore clearly distinguishable from endogenously produced cellular S1P and Sph. Clearance of both C17-S1P and C17-Sph showed similar kinetics compared to their natural C18-analogs (Fig. 2C, D). C17-Sph was again more rapidly metabolized than C17-S1P. A significant conversion of C17-Sph to C17-S1P was not detected. But conversion of C17-S1P to C17-Sph was observed intra and extracellularly, ranging between 4 and 10 pmol/5×10^6 cells and 1–2% of the amount of C17-S1P in the supernatant.

Cellular Uptake of Sph

The slower metabolism of S1P compared to Sph and the partial conversion of S1P to Sph but not vice versa strengthened the possibility that dephosphorylation of extracellular S1P and cellular uptake of resulting Sph may be required for their clearance. Since no cellular accumulation of Sph was observed within 15 min to 8 h (Fig. 2A–D), short-term incubations of 1–20 min with added Sph were performed. A significant accumulation of cellular Sph was found already 1 min after addition of extracellular Sph (Fig. 3A). Sph uptake and clearance was more efficient in suspension than with adherent cells (Figs. 2B, 3A). Cellular accumulation was transient and reached normal levels again after 20 min. Sph uptake and accumulation was an active process and did not occur at 4°C (Fig. 3B). HTC_4 cell incubations with C17-Sph confirmed the transient uptake of Sph (Fig. 3C). The observed early and transient Sph accumulation was therefore mediated by an uptake of extracellular Sph and not by endogenous cellular production. Uptake of C17-Sph was blocked at 4°C (Fig. 3D). Similar results were achieved by incubating HTC_4 cells with fluorescein-labeled S1P and Sph (S1P/Sph-FITC). S1P-FITC and Sph-FITC were very stable even after overnight incubation in 2 ml medium with 5×10^5 HTC_4 cells (Supplementary Fig. 1A).

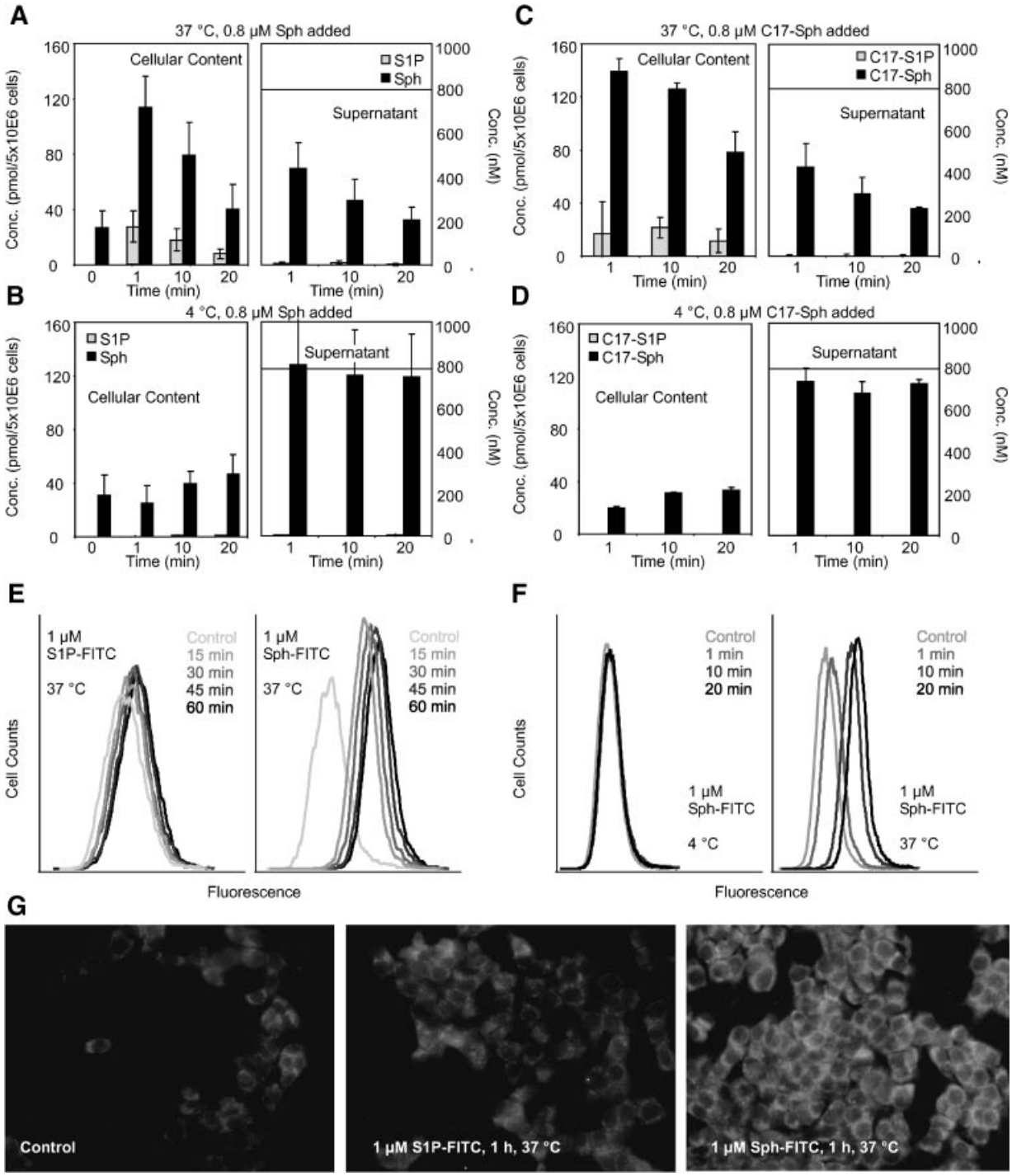

Fig. 3. Cellular uptake of Sph, but not S1P. 1×10^6 HTC_4 cells were incubated in 1 ml medium with 800 nM Sph for 1–20 min in suspension at 37°C (**A**) or at 4°C (**B**). Additional incubations were performed with C17-Sph for 1–20 min at 37°C (**C**) or at 4°C (**D**). Subsequently the amount of S1P, Sph, C17-S1P, and C17-Sph in cells (**left**) and in the medium (**right**) was determined by HPLC. Means of two–four independent experiments including standard errors are shown. **E**: FACS-analysis of 2×10^5 HTC_4 cells incubated with 180 µl of 1 µM S1P-FITC (left) and 1 µM Sph-FITC (right) for 15–60 min at 37°C. **F**: FACS-analysis of 2×10^5 HTC_4 cells treated with 180 µl of 1 µM Sph-FITC at 4°C (left) and at 37°C (right) for 1–20 min. The fluorescence intensities compared to non-treated control cells of one out of three independent experiments are shown. **G**: Fluorescence microscopy of untreated HTC_4 cells (Control) and 1 h after addition of 0.5 ml of 1 µM S1P-FITC or Sph-FITC. One representative picture of three independent experiments is shown.

Only minor dephosphorylation of S1P-FITC was found after 15 h incubation with HTC_4 cells (Supplementary Fig. 1A). A major shift in cellular fluorescence using flow cytometry was only observed after incubation with Sph-FITC, but not with S1P-FITC (Fig. 3E). Sph-FITC uptake was rapid with a 2.3-fold shift after 15 min, and further increased slightly by 0.4-fold after 60 min. Sph-FITC uptake was specific and did not occur on ice (Fig. 3F). Cellular incorporation of Sph-FITC was already visible after 1 min at 37°C, but the majority of Sph-FITC was taken up in 10 min (Fig. 3F). Fluorescence microscopy revealed that Sph-FITC was primarily localized intracellularly in the perinuclear space (Fig. 3G). An increase in fluorescence over basal values was only visible in Sph-FITC-treated cells and not in untreated or S1P-FITC-treated cells. HPLC analysis revealed that incorporated Sph was converted by HTC_4 cells to an unidentified metabolite in 30 min (Supplementary Fig. 1B). Incorporation and metabolism of extracellular Sph-FITC stopped with the accumulation of this metabolite, meaning that the remaining amount of extracellular Sph-FITC was not incorporated and metabolized, and therefore stayed stable outside the cells (Supplementary Fig. 1A, B).

Sub-Cellular Requirements for Metabolic Conversion of S1P and Sph

HTC_4 cells were homogenized and separated into membrane, cytosolic, and nuclear fractions. The amount of endogenous S1P and Sph in all cellular fractions was less than 5 pmol/sample. S1P and Sph were added to each fraction at a concentration of 1 μM and incubated at 37°C for 4 h. Subsequent analysis of sphingolipids displayed a major dephosphorylation activity for S1P to Sph in all cellular fractions (Fig. 4A). Besides S1P and Sph, an additional unidentified metabolite was observed by HPLC analysis after addition of S1P, but not Sph (Supplementary Fig. 2). Added Sph remained untouched in all cellular fractions (Fig. 4B). Notably, under the specific conditions used,

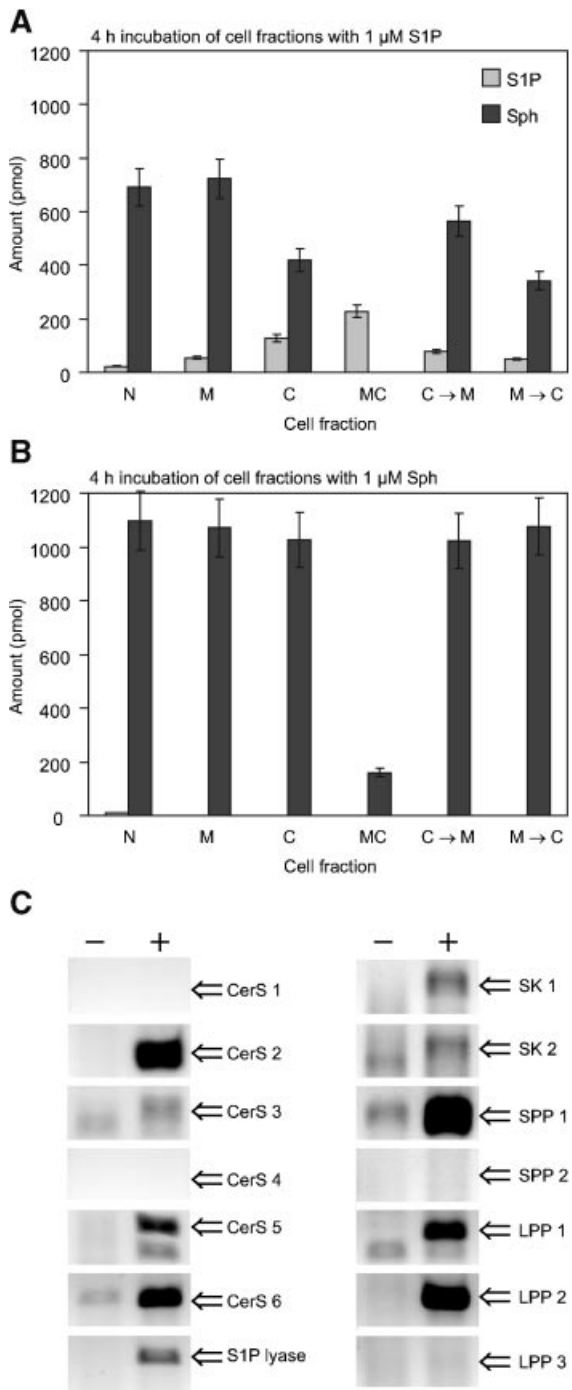

Fig. 4. S1P and Sph metabolism of different HTC_4 cell fractions. 4×10^7 HTC_4 cells were separated into nuclear (N), cell membrane (M), and cytosolic (C) fractions, and two equal parts were incubated in 1 ml PBS for 4 h with 1 nmol/ml S1P (**A**) and Sph (**B**). Furthermore cell membrane and cytosolic fractions from 2×10^7 HTC_4 cells for each single incubation were combined (MC) or successively (M → C or C → M) incubated in 1 ml PBS for 4 (4 + 4) h after initial addition of 1 nmol/ml S1P (A) and Sph (B). After lipid extraction the concentration of S1P and Sph were determined. Each experiment was done three times. Error bars represent standard errors of the validated detection method. **C**: RT-PCR analysis of the expression of ceramide synthases (CerS) type 1–6, S1P-lyase, sphingosine kinases (SKs) type 1 and 2, S1P phosphatases (SPP) type 1 and 2, and lipid phosphate phosphatases (LPP) type 1–3 in HTC_4 cells. Negative controls were performed without addition of reverse transcriptase during cDNA synthesis.

S1P and Sph were only further metabolized when membrane and cytosolic fractions were combined (Fig. 4A, B). Subsequent incubation of S1P and Sph with membrane and cytosolic fraction or vice versa did not result in further metabolic conversion of both compounds under the specific conditions of this experiment (Fig. 4A, B), indicating that membrane and cytosolic enzymes acted jointly to metabolize sphingolipids. In contrast to S1P-incubation with single cellular fractions, the combined metabolic activity of membrane and cytosolic fractions on S1P did not lead to accumulation of Sph (Fig. 4A). Since no protease inhibitors or different buffer conditions were used, certain Sph or S1P-metabolizing enzymes like the S1P-lyase or Sph kinases may not have been active in this particular setting. This experiment therefore does not exclude the existence of other degrading pathways under physiological conditions. RT-PCR revealed that ceramide synthases type 2, 3, 5, and 6, S1P-lyase, Sph kinases type 1 and 2, S1P phosphatase 1, and lipid phosphate phosphatases type 1 and 2 were expressed in HTC_4 cells (Fig. 4C).

Role of Sphingosine Kinase, Ceramide Synthase, and S1P-Lyase for Clearance of Extracellular S1P and Sph

Intracellular Sph can either be phosphorylated to S1P and subsequently degraded to phosphoethanolamine and hexadecenal by the S1P-lyase or metabolized to ceramide by the ceramide synthase. To see the relevance of both metabolic pathways for the observed clearance of extracellular S1P and Sph, we tested the influence of the Sph kinase inhibitor dimethylsphingosine (DMS) and the vitamin B6 antagonist and S1P-lyase inhibitor 4-deoxypyridoxine (DOP) on the metabolism of extracellular S1P and Sph. Overnight incubation of HTC_4 cells treated with 300 nM S1P or Sph showed no difference in their capacity to deplete extracellularly added S1P or Sph from the supernatant with or without 10 μM DMS (Fig. 5A). Even short-term kinetics for 2 h did not reveal any significant differences with or without prior addition of 10 μM DMS regarding clearance of extracellular S1P by HTC_4 cells or HEK293 cells (Fig. 5B). The S1P-lyase inhibitor DOP also had no effect on clearance of extracellular S1P. Over a 2 h period extracellular S1P was metabolized by HTC_4 cells treated with 0.5 mM DOP to the same extent control cells did (Fig. 5C). Intracellular S1P and Sph levels remained unchanged (data not shown). DOP-treated primary mouse splenocytes however did show increased cellular S1P levels after 2 h incubation in the presence of 1 μM Sph which indicated that DOP was indeed capable to inhibit the S1P-lyase under the conditions used (Fig. 5D). The active phosphatase inhibitor sodium orthovanadate used before (Fig. 1E) was not influencing the cellular S1P-level (Fig. 5D). Sodium orthovanadate was shown before to inhibit intracellular protein tyrosine phosphatases at millimolar concentrations that were used [Cuncic et al., 1999], and it is an inhibitor of lipid phosphatases as well [Ogawa et al., 2003]. Overnight incubation with the ceramide synthase inhibitor fumonisin B1 also did not prevent clearance of exogenous S1P or Sph (Fig. 5E). The toxin however worked well and showed the expected increase in cellular DH-Sph levels (Fig. 5E). S1P-levels were unchanged and hardly detectable in all cells, and intracellular DH-S1P levels were slightly increased from 29 ± 4 to 47 ± 7 pmol/5×10^6 cells in all fumonisin B1-treated cells (data not shown).

Fig. 5. Effect of different inhibitors of the sphingolipid metabolism on S1P and Sph metabolism. **A**: Extracellular (**left**) and intracellular (**right**) concentration of S1P and Sph after overnight incubation of 5×10^5 HTC_4 cells in 10 ml medium treated with 300 nM S1P and Sph in the presence of 10 μM of the SK inhibitor DMS when indicated. The experiment was performed twice. Error bars represent standard errors of the validated detection method. **B**: Short-term kinetics of clearance of 300 nM extracellular S1P in 10 ml medium by 5×10^6 untreated HEK293 cells (left) and by 5×10^6 HEK293 cells treated with 10 μM DMS (right). The experiment was performed twice. Error bars represent standard errors of the validated detection method. **C**: Short-term kinetics of clearance of 300 nM extracellular S1P in 2 ml medium by 8×10^5 HTC_4 cells untreated and treated with 0.5 mM of the vitamin B_6-antagonist and S1P-lyase inhibitor DOP. The experiment was performed three times. Error bars represent standard errors of the validated detection method. **D**: 5×10^6 primary mouse lymphocytes were incubated for 2 h in 1 ml medium with 1 μM Sph in the presence or absence of 0.5 mM DOP and 1 mM SOV as indicated. After lipid extraction the concentration of cellular S1P and Sph present in 5×10^6 E6 cells was determined. Means of two independent experiments including standard errors are shown. **E**: Extracellular (left) and intracellular (right) concentration of Sph, DH-Sph, and S1P respectively after overnight incubation of HTC_4 cell cultures treated with 300 nM S1P and Sph in the presence of 10 μM of the ceramide synthase inhibitor fumonisin B1 (FuB1) when indicated. The respective cellular content of S1P was equivalent to that shown in Figure 1B. Each experiment was done twice. Error bars represent standard errors of the validated detection method.

S1P Degradation by Primary Mouse Splenocytes

Cell suspensions of lymphocytes isolated from mouse spleen were incubated for 6 h with 0.5 μM S1P or 1 μM Sph. Subsequent analysis of S1P, DH-S1P, and Sph levels in medium manifested a reduction of exogenously added S1P and Sph after the 6 h incubation period (Fig. 6A). Clearance of S1P was blocked by the phosphatase inhibitor sodium orthovanadate (Fig. 6A).

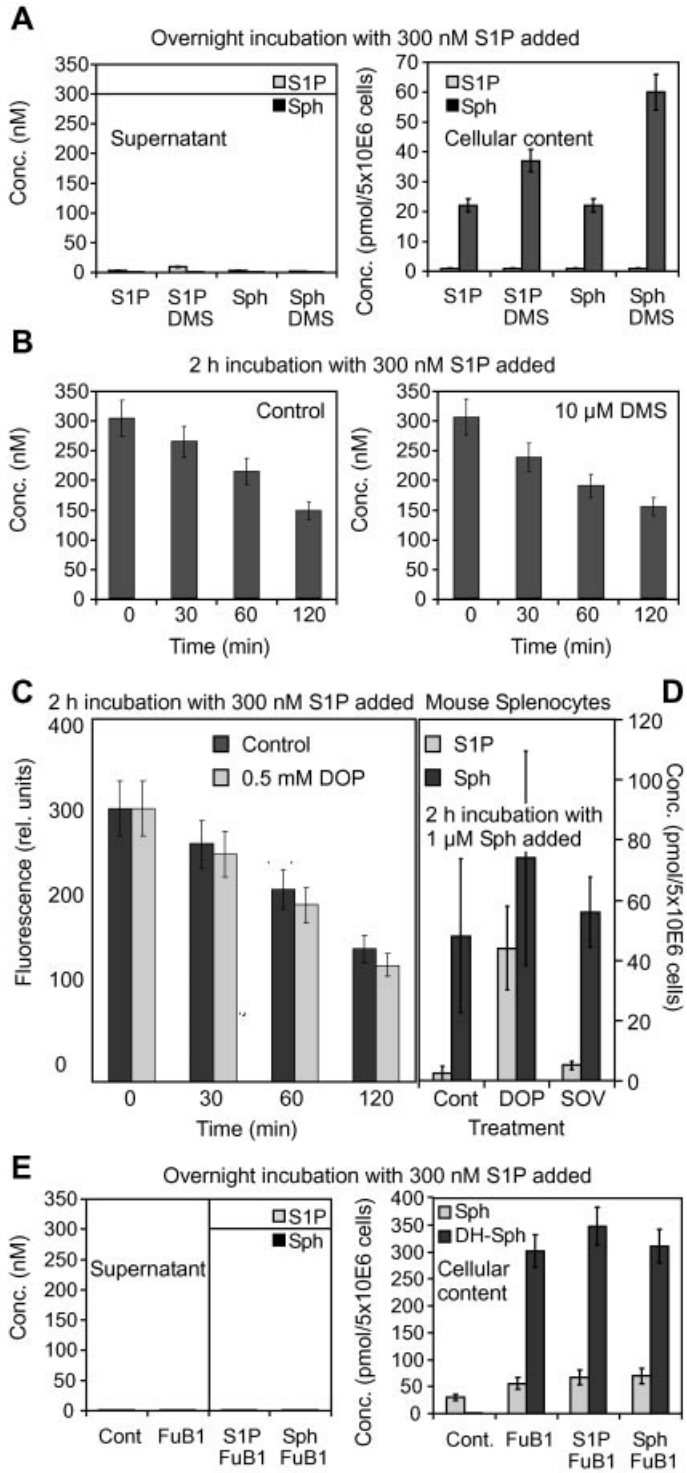

Fig. 5.

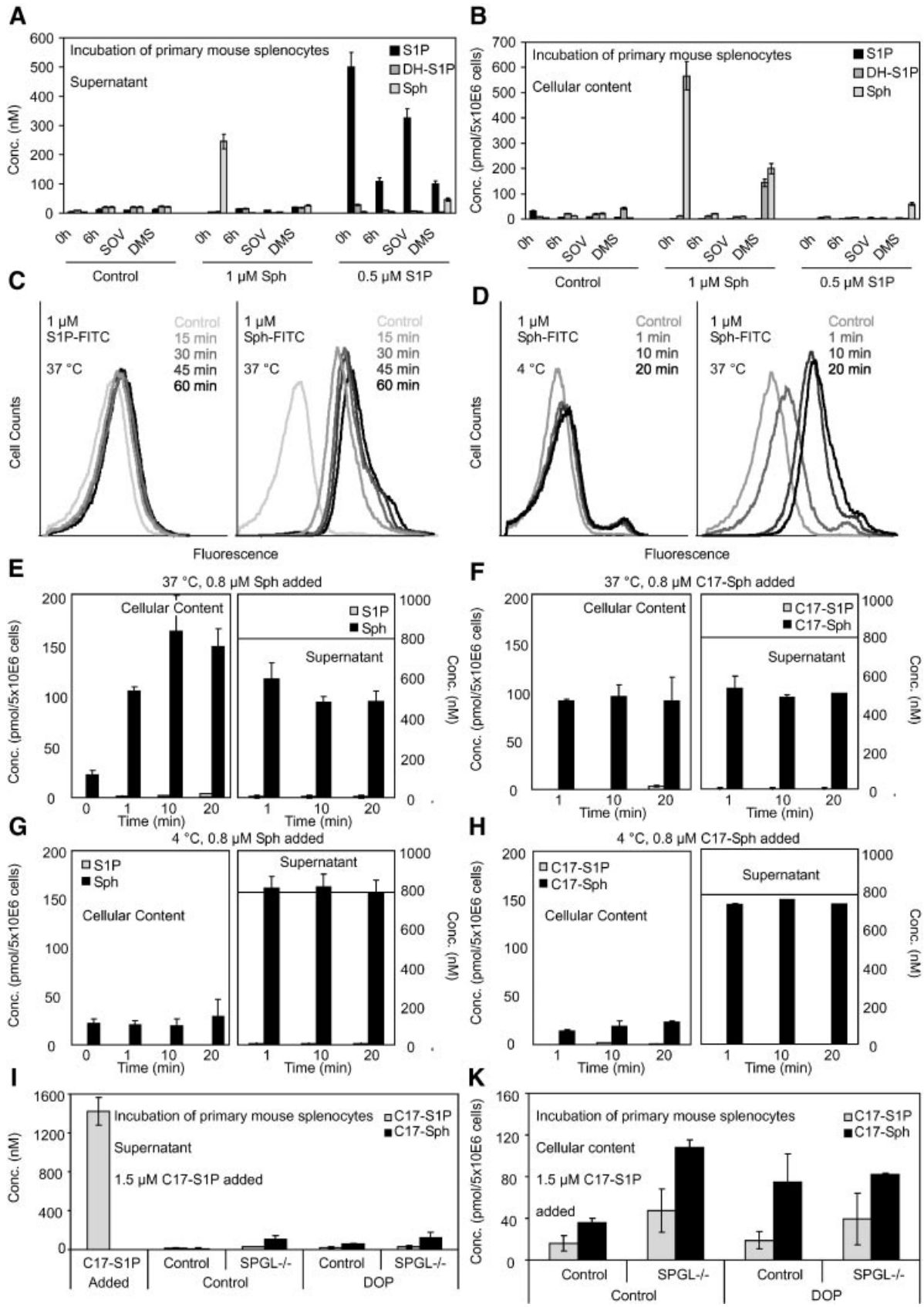
A
Incubation of primary mouse splenocytes
Supernatant
S1P
DH-S1P
Sph
Conc. (nM)
0h 6h SOV DMS 0h 6h SOV DMS 0h 6h SOV DMS
Control
1 µM Sph
0.5 µM S1P
B
Incubation of primary mouse splenocytes
Cellular content
S1P
DH-S1P
Sph
Conc. (pmol/5x10E6 cells)
Control
1 µM Sph
0.5 µM S1P
C
1 µM S1P-FITC
37 °C
Control
15 min
30 min
45 min
60 min
1 µM Sph-FITC
37 °C
Cell Counts
Fluorescence
D
1 µM Sph-FITC
4 °C
Control
1 min
10 min
20 min
1 µM Sph-FITC
37 °C
Cell Counts
Fluorescence
E
37 °C, 0.8 µM Sph added
Cellular Content
S1P
Sph
Supernatant
Conc. (pmol/5x10E6 cells)
Conc. (nM)
Time (min)
F
37 °C, 0.8 µM C17-Sph added
Cellular Content
C17-S1P
C17-Sph
Supernatant
Conc. (pmol/5x10E6 cells)
Conc. (nM)
Time (min)
G
4 °C, 0.8 µM Sph added
S1P
Sph
Cellular Content
Supernatant
Conc. (pmol/5x10E6 cells)
Conc. (nM)
Time (min)
H
4 °C, 0.8 µM C17-Sph added
C17-S1P
C17-Sph
Cellular Content
Supernatant
Conc. (pmol/5x10E6 cells)
Conc. (nM)
Time (min)
I
Incubation of primary mouse splenocytes
Supernatant
1.5 µM C17-S1P added
C17-S1P
C17-Sph
Conc. (nM)
C17-S1P Added
Control
SPGL-/-
Control
SPGL-/-
Control
DOP
K
Incubation of primary mouse splenocytes
Cellular content
1.5 µM C17-S1P added
C17-S1P
C17-Sph
Conc. (pmol/5x10E6 cells)
Control
SPGL-/-
Control
SPGL-/-
Control
DOP

Fig. 6.

The Sph kinase inhibitor DMS had no effect on extracellular S1P degradation (Fig. 6A). Both inhibitors had no effect on Sph degradation (Fig. 6A). Intracellular S1P levels were hardly detectable and unchanged (Fig. 6B). Sph however was rapidly taken up by primary mouse splenocytes and metabolized (Fig. 6B). Sph uptake was also observed with Sph-FITC by flow cytometry (Fig. 6C). S1P-FITC did not accumulate in splenocytes. Incorporation of Sph-FITC was only visible after incubation at 37°C and not at 4°C (Fig. 6D). Rapid uptake and accumulation of Sph was also shown by HPLC-analysis (Fig. 6E). Uptake and accumulation of C17-Sph was similar to the natural sphingolipid (Fig. 6F). Cellular uptake and accumulation of Sph and C17-Sph did not occur at 4°C (Fig. 6G, H). Accordingly degradation of extracellular S1P and Sph did not take place (Fig. 6G, H). DMS treatment led to a slight increase in intracellular Sph levels after S1P addition (Fig. 6B). Exogenously added Sph provoked an increase in Sph and DH-S1P levels in the presence of DMS (Fig. 6B). The observed increase in DH-S1P may be due to competitive inhibition of DH-Sph acylation by DMS, which consequently would increase DH-Sph levels above the Michaelis constant K_M for Sph kinase 2. To further demonstrate that rephosphorylation of Sph with Sph kinase and degradation of the resulting S1P by the S1P-lyase did not play a role for clearance of extracellular S1P, lymphocytes from DOP-treated mice and S1P-lyase deficient mice were incubated with added C17-S1P. It was shown recently that the S1P-lyase is active in lymphoid tissues [Schwab et al., 2005]. This experiment revealed that even S1P-lyase deficient lymphocytes were able to metabolize exogenously added C17-S1P (Fig. 6I). Treatment with DOP also did not block the metabolism of extracellular S1P (Fig. 6I). An increase in C17-Sph was observed in S1P-lyase deficient lymphocytes and in DOP-treated lymphocytes after incubation with C17-S1P (Fig. 6K). Cellular C17-S1P levels were increased only in S1P-lyase deficient lymphocytes (Fig. 6K). Endogenous S1P levels were 2 ± 2 pmol/1×10^6 cells in wild-type control splenocytes and 140 ± 90 pmol/1×10^6 cells in S1P-lyase deficient splenocytes. Accumulated endogenous cellular S1P and Sph levels in S1P-lyase deficient splenocytes were much more stable than exogenously added C17-S1P (Supplementary Fig. 3). Whereas 1.5 μM extracellularly added C17-S1P was virtually cleared by S1P-lyase deficient splenocytes in 4 h (Fig. 6I), the amount of endogenously accumulated cellular S1P and Sph was reduced only four–sixfold after 15 h incubation (Supplementary Fig. 3).

In Vivo and Ex Vivo Degradation of S1P in Mouse Blood

One milligram of S1P per kilogram bodyweight was intravenously injected into the tail vein of wild-type C57BL/6 mice. Samples of heparinized plasma were taken from mice that were sacrificed after 1, 4, 6, 8, 15, and 30 min. Subsequent analysis of sphingolipids manifested a rapid and transient increase in S1P plasma levels whereas DH-S1P levels remained unchanged (Fig. 7A). Compared to vehicle-injected control mice, injection of S1P increased the in vivo plasma concentration from 1 μM to 2.5 μM S1P after 1 min (Fig. 7A). Plasma concentration of S1P reached basal levels again after 15–30 min (Fig. 7A). We did not observe any significant increase in DH-S1P levels which leveled off at approximately 250 nM (Fig. 7A). When 3 μM S1P was added to mouse blood ex

Fig. 6. Cellular uptake of Sph, and clearance of S1P and Sph by primary mouse splenocytes. **A**: Extracellular and (**B**) intracellular concentrations of S1P, DH-S1P, and Sph of primary mouse splenocyte cultures (5×10^6 cells in 1 ml medium) untreated (Control) and treated with 1 μM Sph or 0.5 μM S1P. Values after 1 min and after 6 h without and with addition of 1 mM of the phosphatase inhibitor SOV and 10 μM of the SK inhibitor DMS when indicated are shown. Each experiment was done twice. Error bars represent standard errors of the validated detection method. **C**: FACS-analysis of 1×10^6 mouse splenocytes incubated in 180 μl medium with 1 μM S1P-FITC (**left**) and 1 μM Sph-FITC (**right**) for 15–60 min at 37°C. **D**: FACS-analysis of 1×10^6 mouse splenocytes in 180 μl medium treated with 1 μM Sph-FITC at 4°C (left) and at 37°C (right) for 1–20 min. The fluorescence intensities compared to non-treated control cells of one out of three independent experiments are shown. **E–H**: 5×10^6 mouse splenocytes were incubated in 1 ml medium with 800 nM Sph for 1–20 min at 37°C (E) or at 4°C (G). Additional incubations were performed with C17-Sph for 1–20 min at 37°C (F) or at 4°C (H). Subsequently the amount of S1P, Sph, C17-S1P, and C17-Sph in cells (left) and in the medium (right) was determined by HPLC. Means of two independent experiments including standard errors are shown. **I**: Extracellular and (**K**) intracellular concentrations of C17-S1P and C17-Sph of primary mouse splenocyte cultures (5×10^6 cells in 1 ml medium) from wild-type SW mice (Control) and S1P-lyase deficient mice ($SPGL^{-/-}$) untreated (Control) and treated with 0.5 mM DOP 4 h after addition of 1.5 μM C17-S1P. Means of two independent experiments including standard errors are shown.

vivo and incubated for 8 h at 37°C, the plasma concentration increased to 2.3 μM and went down again to nearly basal levels of 1.1 μM (Fig. 7B). Clearance of 1 μM exogenously added S1P was also observed with mouse blood cells that were incubated in RPMI supplemented with 10% FCS over an 8 h period (Fig. 7C). In contrast to the observed in vivo clearance of intravenously injected S1P (Fig. 7A), depletion of added S1P in the supernatant of whole blood (Fig. 7B) or blood cells that were resuspended in medium (Fig. 7C) was much slower. Basal S1P levels in mouse blood showed only a minor increase even after prolonged incubation at 37°C for 4 h (Fig. 7D).

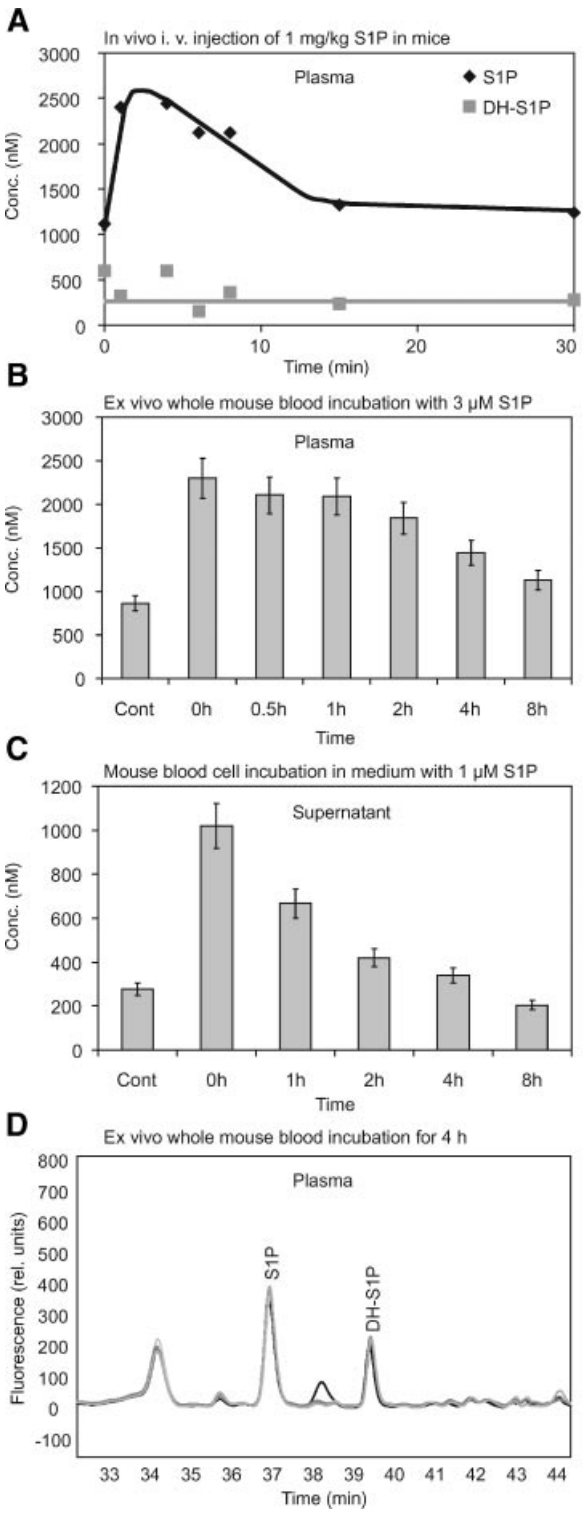

DISCUSSION

S1P is constitutively present in blood and released by various cell types including thrombocytes, mast cells, and erythrocytes [Yatomi et al., 1997; Yatomi et al., 2000; Ruwisch et al., 2001; Jolly et al., 2004; Hänel et al., 2007]. Cellular pathways for synthesis and metabolism of Sph and its phosphorylated relative S1P are well defined [Saba and Hla, 2004]. However little is known about the regulation of extracellular S1P. Identification of five G protein-coupled receptors that are specific for S1P highlights its role as a potent extracellular mediator in various biological systems including immune surveillance. Genetically engineered mouse models clearly indicate the importance of the $S1P_1$ receptor in lymphocyte circulation and the role for blood-borne S1P in lymphocyte egress from spleen and thymus [Allende et al., 2004; Matloubian et al., 2004; Gräler et al., 2005; Pappu et al., 2007].

We established an HPLC-based analysis of sphingolipids to examine the fate of exogenously added extracellular S1P in wild-type

Fig. 7. S1P clearance by primary mouse blood cells. **A**: In vivo clearance of 1 mg/kg intravenously injected S1P in C57BL/6 mice. Plasma samples taken at indicated times after S1P injection of one out of two similar experiments are shown. **B**: Ex vivo clearance of 3 μM exogenously added S1P in 300 μl of mouse blood. Heparinized mouse blood samples were incubated for the indicated period of time at 37°C. Subsequently the resulting plasma samples were analyzed for their S1P content. The experiment was done twice, error bars represent standard errors of the validated detection method. **C**: 300 μl of precipitated heparinized mouse blood cells were incubated in 300 μl RPMI medium supplemented with 1 μM S1P. Medium samples were taken at indicated time points and analyzed for their S1P contents. The experiment was done twice, error bars represent standard errors of the validated detection method. **D**: Heparinized mouse blood was incubated at 37°C ex vivo. Chromatograms of plasma samples taken after 0 h (black), 1 h (dark gray), 2 h (medium gray), and 4 h (light gray) are shown. One out of two similar experiments is shown.

C57BL/6 mice and in cell cultures of primary mouse splenocytes, blood cells, and different cell lines [Andréani and Gräler, 2006]. In contrast to other HPLC-based methods described [Ruwisch et al., 2001; Butter et al., 2005], the detection of sphingolipids in various biological samples at the same time made it possible to pursue the conversion of S1P to Sph and vice versa [Andréani and Gräler, 2006]. Quantification occurred directly and independently from defined enzymatic processes, which is a major advantage compared to assays using radioactively labeled sphingolipids [Andréani and Gräler, 2006]. Cellular uptake of Sph, but not S1P was confirmed by flow cytometry and fluorescence microscopy using fluorescein-labeled S1P and Sph (Figs. 3E–G, 6C–D). The fluorescein-labeled sphingolipids resembled the results obtained with natural S1P and Sph (Figs. 3A–D, 6E–H). Furthermore S1P-FITC was able to induce a specific increase in the intracellular calcium concentration of HTC_4 cells that were transduced with the $S1P_3$ receptor (data not shown). S1P-FITC therefore retained its activity as an active ligand for the $S1P_3$ receptor. Contribution of endogenous sphingolipid production and conversion was also distinguishable from exogenously added S1P and Sph using synthetic C17-S1P and C17-Sph derivatives (Figs. 3C–D, 6F, H, I, K).

HPLC-analysis of S1P-FITC and Sph-FITC resulted in a double-peak for both substances, whereas FITC alone eluted in a single peak (Supplementary Fig. 1A, B). The occurrence of double-peaks cannot be easily explained, since both substances have the natural D-erythro stereochemistry. One possible reason however could be the incidence of nitrogen inversion at the amino group that covalently bound FITC, which would also explain the observed peak coalescence (Supplementary Fig. 1A, B). The three-dimensional position of the FITC label in relation to the distant polar head group of S1P and Sph may influence the affinity to the reversed phase, and therefore result in the observed double-peak. Fluorescent labeling at the inherent amino group of S1P and Sph may not result in double-peaks because of the close proximity of the fluorescent dye to the polar head group, which may not change the binding affinity to the reversed phase in response to nitrogen inversion.

The presented results support the idea that extracellular S1P needs to be dephosphorylated by cells in order to be taken up as Sph which is rapidly metabolized, a process that is not altered by DMS, DOP, or fumonisin B1. This observation is in line with previous data on the metabolism of exogenous DH-S1P by human skin fibroblasts, also revealing an active dephosphorylation process [Van Veldhoven and Mannaerts, 1994]. In the presence of the phosphatase inhibitor sodium orthovanadate, extracellular S1P was completely stable even after overnight incubation with HTC_4 cells (Fig. 1E). Importantly S1P did not significantly accumulate within the cells, which indicated that S1P was not efficiently taken up by cells in its phosphorylated state.

Exogenously added C17-S1P was efficiently degraded by S1P-lyase deficient splenocytes (Fig. 6I), whereas endogenously accumulated cellular S1P and Sph were rather stable (Supplementary Fig. 3). Even overnight incubation of S1P-lyase deficient splenocytes did not result in complete clearance of endogenous cellular S1P and Sph levels (Supplementary Fig. 3). Thus metabolism of endogenous cellular and exogenously added S1P and Sph are different and separate from each other. The reason for this discrimination may be a different cellular localization of these sphingolipids. The combined activity of membrane and cytosolic fractions for S1P and Sph degradation suggests that the intracellular location of these sphingolipids is important for their stability (Fig. 4). Since S1P-lyase deficiency results in cellular accumulation of S1P and Sph (Supplementary Fig. 3), this enzyme appears to be important for degradation of endogenous cellular S1P and Sph. But S1P-lyase deficiency did not inhibit the degradation of extracellular C17-S1P (Fig. 6I). Thus cellular and extracellular S1P are handled differently. Degradation of cellular S1P appears to be highly dependent on S1P-lyase, whereas clearance of extracellular S1P was mainly S1P-lyase independent.

Metabolism of extracellular S1P and Sph by primary mouse splenocytes and other cells of different sources is a novel finding that points to an important mechanism for clearance of excess amounts of extracellular S1P. Notably all cultured cell lines as well as primary mouse lymphocytes metabolized exogenously added S1P and Sph, indicating that S1P and Sph degradation is a rather ubiquitous process (Fig. 1A). Production and secretion of S1P was below the quantification limit of 10 pmol/mg of

the HPLC method that was used (Fig. 1A). It is therefore reasonable to suggest that extracellular S1P and Sph concentrations in the local environment of SLOs and peripheral tissues are kept low. In fact S1P and Sph levels in different mouse tissues including spleen, thymus, lymph nodes, kidney, heart, liver, and others were below 10 pmol/mg tissue (Supplementary Fig. 4).

The coordinated activity of membrane and cytosolic enzymes in Sph metabolism points to a well-controlled multi-step process (Fig. 4). Recent studies of S1P and Sph metabolism in human umbilical vein endothelial cells (HUVEC) indicate that ceramides can serve as a sink for access amount of bioactive Sph [Aoki et al., 2005]. Inhibition of the ceramide synthase however did not prevent the observed clearance of extracellular S1P and Sph (Fig. 5E). Our data indicate that neither S1P-lyase nor ceramide synthase are involved in the observed clearance of extracellular S1P and Sph. Clearance of extracellular S1P requires its dephosphorylation to Sph (Fig. 1C, E). Sph is therefore the basic metabolite in extracellular S1P metabolism.

The putative role of S1P receptors, especially $S1P_1$ as the most ubiquitously expressed member of the S1P receptor family, was evaluated by incubating $S1P_1$ receptor expressing HTC_4 cells and plain HTC_4 cells devoid of any S1P receptors with 300 nM S1P. Both cell lines degraded S1P at a similar rate shown in Fig. 2A (data not shown). Therefore a requirement for S1P receptors for clearance of extracellular S1P can be excluded. Furthermore the expression of the $S1P_1$ receptor had neither a stimulating nor a retarding effect on S1P metabolism by HTC_4 cells. Thus S1P receptors do not seem to play a role for clearance of extracellular S1P.

We have recently shown that human erythrocytes are able to incorporate, store, and protect S1P in blood [Hänel et al., 2007]. Here we demonstrate that mouse blood cells have similar capabilities. S1P-levels were stable in whole mouse blood (Fig. 7D), and exogenously added S1P was cleared from plasma (Fig. 7B) and medium (Fig. 7C). Clearance of extracellularly added S1P however took several hours (Fig. 7B, C), whereas in vivo clearance of intravenously injected S1P from mouse plasma was accomplished in 15 min (Fig. 7A). Although in vivo clearance of S1P in the plasma may also be realized through redistribution into peripheral tissues, the presented in vitro data would at least suggest that metabolic conversion of S1P, for example, by vascular endothelial cells may also be involved. Nevertheless mouse blood samples were able to maintain their endogenous S1P levels, although exogenously added S1P was completely cleared from plasma over time (Fig. 7B–D). Setting up of a steady-state condition between degradation and production of blood-borne S1P may be an explanation for this observation which is currently under investigation. The extraordinary high levels of extracellular S1P in mouse blood compared to other local tissue environments also identify blood as a specialized compartment with regard to S1P metabolism.

Based on these findings we propose a model with altered S1P metabolism depending on the local environment and its condition. In SLOs and peripheral tissues the extracellular S1P concentration is kept low due to the metabolic activity of lymphocytes and tissue cells. Stimulation of cells like thrombocytes and mast cells in disease states such as injuries or infections induce a local and transient release of S1P. This activates S1P receptors expressed on the cell surface of lymphocytes and other cells which facilitates wound healing or supports an immune response. In blood however S1P metabolism by vascular endothelial cells and S1P production by erythrocytes constitute a steady-state condition. This balance is shifted in certain disease patterns [Schwab et al., 2005]. Tools for manipulating blood S1P levels will be helpful to further investigate the in vivo role of S1P.

ACKNOWLEDGMENTS

The authors thank Anika Münk for her excellent technical assistance. This work was supported by the German Research Foundation (DFG), grant GR-1943/1-3 of the Emmy Noether Program.

REFERENCES

Allende ML, Dreier JL, Mandala S, Proia RL. 2004. Expression of the sphingosine 1-phosphate receptor, S1P1, on T-cells controls thymic emigration. J Biol Chem 279:15396–15401.

An S, Bleu T, Huang W, Hallmark OG, Coughlin SR, Goetzl EJ. 1997. Identification of cDNAs encoding two G

protein-coupled receptors for lysosphingolipids. FEBS Lett 417:279–282.

Andréani P, Gräler MH. 2006. Comparative quantification of sphingolipids and analogs in biological samples by high-performance liquid chromatography after chloroform extraction. Anal Biochem 358:239–246.

Aoki S, Yatomi Y, Ohta M, Osada M, Kazama F, Satoh K, Nakahara K, Ozaki Y. 2005. Sphingosine 1-phosphate-related metabolism in the blood vessel. J Biochem (Tokyo) 138:47–55.

Butter JJ, Koopmans RP, Michel MC. 2005. A rapid and validated HPLC method to quantify sphingosine 1-phosphate in human plasma using solid-phase extraction followed by derivatization with fluorescence detection. J Chromatogr B Analyt Technol Biomed Life Sci 824:65–70.

Chun J, Goetzl EJ, Hla T, Igarashi Y, Lynch KR, Moolenaar W, Pyne S, Tigyi G. 2002. International Union of Pharmacology. XXXIV. Lysophospholipid receptor nomenclature. Pharmacol Rev 54:265–269.

Cummings RJ, Parinandi NL, Zaiman A, Wang L, Usatyuk PV, Garcia JG, Natarajan V. 2002. Phospholipase D activation by sphingosine 1-phosphate regulates interleukin-8 secretion in human bronchial epithelial cells. J Biol Chem 277:30227–30235.

Cuncic C, Desmarais S, Detich N, Tracey AS, Gresser MJ, Ramachandran C. 1999. Bis(N,N-dimethylhydroxamido)hydroxooxovanadate inhibition of protein tyrosine phosphatase activity in intact cells: Comparison with vanadate. Biochem Pharmacol 58:1859–1867.

Cuvillier O, Pirianov G, Kleuser B, Vanek PG, Coso OA, Gutkind S, Spiegel S. 1996. Suppression of ceramide-mediated programmed cell death by sphingosine-1-phosphate. Nature 381:800–803.

English D, Welch Z, Kovala AT, Harvey K, Volpert OV, Brindley DN, Garcia JG. 2000a. Sphingosine 1-phosphate released from platelets during clotting accounts for the potent endothelial cell chemotactic activity of blood serum and provides a novel link between hemostasis and angiogenesis. FASEB J 14:2255–2265.

English D, Welch Z, Kovala AT, Harvey K, Volpert OV, Brindley DN, Garcia JG. 2000b. Sphingosine 1-phosphate released from platelets during clotting accounts for the potent endothelial cell chemotactic activity of blood serum and provides a novel link between hemostasis and angiogenesis. FASEB J 14:2255–2265.

Gräler M, Goetzl EJ. 2002. Activation-regulated expression and chemotactic function of sphingosine 1-phosphate receptors in mouse splenic T cells. FASEB J 16:1874–1878.

Gräler MH, Goetzl EJ. 2004. The immunosuppressant FTY720 down-regulates sphingosine 1-phosphate G-protein-coupled receptors. FASEB J 18:551–553.

Gräler M, Shankar G, Goetzl EJ. 2002. Cutting edge: Suppression of T cell chemotaxis by sphingosine 1-phosphate. J Immunol 169:4084–4087.

Gräler MH, Huang MC, Watson S, Goetzl EJ. 2005. Immunological effects of transgenic constitutive expression of the type 1 sphingosine 1-phosphate receptor by mouse lymphocytes. J Immunol 174:1997–2003.

Hänel P, Andréani P, Gräler MH. 2007. Erythrocytes store and release sphingosine 1-phosphate in blood. FASEB J 21:1202–1209.

Im DS, Heise CE, Ancellin N, O'Dowd BF, Shei GJ, Heavens RP, Rigby MR, Hla T, Mandala S, McAllister G, George SR, Lynch KR. 2000. Characterization of a novel sphingosine 1-phosphate receptor, Edg-8. J Biol Chem 275:14281–14286.

Jolly PS, Bektas M, Olivera A, Gonzalez-Espinosa C, Proia RL, Rivera J, Milstien S, Spiegel S. 2004. Transactivation of sphingosine-1-phosphate receptors by FcepsilonRI triggering is required for normal mast cell degranulation and chemotaxis. J Exp Med 199:959–970.

Lee MJ, Van Brocklyn JR, Thangada S, Liu CH, Hand AR, Menzeleev R, Spiegel S, Hla T. 1998. Sphingosine-1-phosphate as a ligand for the G protein-coupled receptor EDG-1. Science 279:1552–1555.

Lee H, Goetzl EJ, An S. 2000. Lysophosphatidic acid and sphingosine 1-phosphate stimulate endothelial cell wound healing. Am J Physiol Cell Physiol 278:C612–C618.

Matloubian M, Lo CG, Cinamon G, Lesneski MJ, Xu Y, Brinkmann V, Allende ML, Proia RL, Cyster JG. 2004. Lymphocyte egress from thymus and peripheral lymphoid organs is dependent on S1P receptor 1. Nature 427:355–360.

Meyer zu Heringdorf D, Liliom K, Schaefer M, Danneberg K, Jaggar JH, Tigyi G, Jakobs KH. 2003. Photolysis of intracellular caged sphingosine-1-phosphate causes Ca2+ mobilization independently of G-protein-coupled receptors. FEBS Lett 554:443–449.

Ogawa C, Kihara A, Gokoh M, Igarashi Y. 2003. Identification and characterization of a novel human sphingosine-1-phosphate phosphohydrolase, hS PP2. J Biol Chem 278:1268–1272.

Pappu R, Schwab SR, Cornelissen I, Pereira JP, Regard JB, Xu Y, Camerer E, Zheng YW, Huang Y, Cyster JG, Coughlin SR. 2007. Promotion of lymphocyte egress into blood and lymph by distinct sources of sphingosine-1-phosphate. Science 316:295–298.

Roviezzo F, Del Galdo F, Abbate G, Bucci M, D'Agostino B, Antunes E, De Dominicis G, Parente L, Rossi F, Cirino G, De Palma R. 2004. Human eosinophil chemotaxis and selective in vivo recruitment by sphingosine 1-phosphate. Proc Natl Acad Sci USA 101:11170–11175.

Ruwisch L, Schafer-Korting M, Kleuser B. 2001. An improved high-performance liquid chromatographic method for the determination of sphingosine-1-phosphate in complex biological materials. Naunyn Schmiedebergs Arch Pharmacol 363:358–363.

Saba JD, Hla T. 2004. Point-counterpoint of sphingosine 1-phosphate metabolism. Circ Res 94:724–734.

Schwab SR, Pereira JP, Matloubian M, Xu Y, Huang Y, Cyster JG. 2005. Lymphocyte sequestration through S1P lyase inhibition and disruption of S1P gradients. Science 309:1735–1739.

Van Brocklyn JR, Gräler MH, Bernhardt G, Hobson JP, Lipp M, Spiegel S. 2000. Sphingosine-1-phosphate is a ligand for the G protein-coupled receptor EDG-6. Blood 95:2624–2629.

Van Veldhoven PP. 2005. Sphingosine 1-phosphate lyase deficient mice. Chem Phys Lipids 136:164–165.

Van Veldhoven PP, Mannaerts GP. 1994. Sphinganine 1-phosphate metabolism in cultured skin fibroblasts: Evidence for the existence of a sphingosine phosphatase. Biochem J 299:597–601.

Yatomi Y, Igarashi Y, Yang L, Hisano N, Qi R, Asazuma N, Satoh K, Ozaki Y, Kume S. 1997. Sphingosine 1-phosphate, a bioactive sphingolipid abundantly stored in platelets, is a normal constituent of human plasma and serum. J Biochem (Tokyo) 121:969–973.

Yatomi Y, Ohmori T, Rile G, Kazama F, Okamoto H, Sano T, Satoh K, Kume S, Tigyi G, Igarashi Y, Ozaki Y. 2000. Sphingosine 1-phosphate as a major bioactive lysophospholipid that is released from platelets and interacts with endothelial cells. Blood 96:3431–3438.